Department of condensed matter physics
Přírodovědecká fakulta, Masarykova univerzita, Brno

Physical laboratory 4

Magnetization curve

Task goals

Measurement options:

- *Calibration of the magnetometer with a known sample (nickel plate) – mandatory part.*
- *Changes in magnetization of an iron sample after annealing for different cooling rates.*
- *Comparison of hysteresis loop with magnetic field shielding permeability measurements.*
- *Paramagnetic and diamagnetic susceptibility, anisotropy of diamagnetic susceptibility in graphite.*
- *Magnetocrystal anisotropy – differences in magnetization according to different directions in a crystal.*

Theory

The relationship between magnetic intensity $\boldsymbol{H}$ and magnetic induction $\boldsymbol{B}$ is given by

$$\boldsymbol{B} = \mu_0 \left(\boldsymbol{H} + \boldsymbol{M} \right), \tag{1}$$

where $\boldsymbol{M}$ is the magnetization vector that gives the bulk magnetic moment density. The magnetic moment is then the volume of the sample multiplied by the magnetization

$$\boldsymbol{m} = V \boldsymbol{M}. \tag{2}$$

With the known density of the sample and its mass, we can then easily calculate the total magnetic moment per atom. It is convenient to give the magnetic moment per atom in Bohr magneton units $\mu_B = 9{,}274 \cdot 10^{-24}\,\mathrm{Am}^2$. Paramagnetic and diamagnetic materials at normal temperatures show a linear dependence of magnetization on the external field

$$M = \chi H\ , \tag{3}$$

where χ is the magnetic susceptibility, positive for paramagnetics and negative for diamagnetics. Usually, the susceptibility is very small, in the order of 10^{-4} to 10^{-8}. The relative permeability is equal to $^m u_r = 1 +^c hi$. Ferromagnetic materials exhibit a nonlinear hysteresis dependence as shown in figure 1. The main parameters of the hysteresis loop are the coercive field H_c when the magnetization is zero, the remanent magnetization M_R, and the saturation magnetization. It is then possible to introduce an external field-dependent susceptibility as a derivative of the magnetization

$$\chi = \frac{\mathrm{d}M}{\mathrm{d}H};. \tag{4}$$

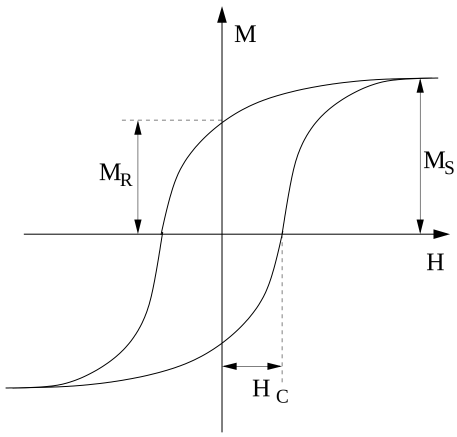

Obrázek 1: Hysteresis dependence.

Often the value is given around the origin, i.e., for zero external magnetic field. This value is important, for example, for the efficiency of transformers, where we are trying to work only in the region of small far-saturation fields.

The change in magnetization of a ferromagnet is due to the movement of the material's domain walls and the volume of the individual domains. Defects in the crystal can slow down the movement of the domain walls and lead to a change in the shape of the hysteresis curve. For example, we can study the effect of the cooling rate of the material on the shape of the hysteresis loop. During rapid cooling (quenching), more defects usually remain in the material than during slow cooling, when the process is closer to thermodynamic equilibrium.

Vibrating sample magnetometer

The vibrating magnetized sample in the vicinity of the coil changes the magnetic field flux, which induces an electromotive voltage in the coil according to Maxwell's equations

$$U = -\frac{\mathrm{d}\Phi}{\mathrm{d}t}. \tag{5}$$

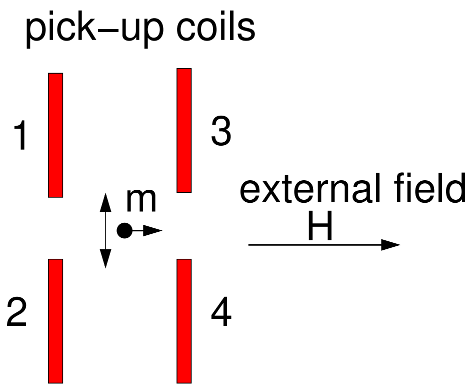

Obrázek 2: Schematic drawing of the relative position of the sample as a magnetic dipole and the detection coil.

A simple quantitative description of our experiment is possible in the approximation where replacing the sample with a magnetic dipole. Furthermore, we will approximate the motion of the sample close to the coil by a harmonic oscillation motion

$$z(t) = z_0 + A_z \cos(\omega t) \tag{6}$$

with amplitude A_z with mean position z_0. The situation is shown in Figure 2. The magnetic field of a magnetic dipole is given by the relation [1, 2]

$$\boldsymbol{B}(\boldsymbol{r}) = \frac{\mu_0}{4\pi r^3}\left[\frac{3(\boldsymbol{r}\cdot\boldsymbol{m})\boldsymbol{r}}{r^2} - \boldsymbol{m}\right] , \tag{7}$$

where $\boldsymbol{r}$ is the position vector relative to the magnetic dipole, $\boldsymbol{m}$ is the magnetic dipole moment, and μ_0 is the vacuum permeability. The real arrangement uses four identical coils, denoted from 1 to 4. Consider first the magnetic flux through coil 1

$$\Phi_1(z(t)) = \int_{S_1} \boldsymbol{n}\cdot\boldsymbol{B}(\boldsymbol{r})\mathrm{d}^2\boldsymbol{r};, \tag{8}$$

where the integration is over the surface of the coil.

This magnetic flux depends on the dimensions and number of turns of the coil and the position of the sample and is directly proportional to the magnetic moment of the sample m. The quantitative calculation of the magnetic flux is quite challenging; for small sample deflections, we can approximate the dependence on the sample deflection by a Taylor expansion to the first order.

$$\Phi_1(z(t)) \approx m\left[-C_0 - C_1 z(t)\right] . \tag{9}$$

According the symmetry of the other coils their particular fluxes are

$$\Phi_2(z(t)) \approx m\left[-C_0 + C_1 z(t)\right] , \ \Phi_3(z(t)) \approx m\left[C_0 + C_1 z(t)\right] , \ \Phi_4(z(t)) \approx m\left[C_0 - C_1 z(t)\right] . \tag{10}$$

The resulting arrangement engages coils 1 and 4 with reversed polarity compared to coils 2 and 3, thus adding up the changes in magnetic flux in each coil. For the magnetic flux through the coil assembly

$$\Phi(t) = -\Phi_1(t) + \Phi_2(t) + \Phi_3(t) - \Phi_4(t) = 4mC_1A_z\cos(\omega t). \tag{11}$$

To determine the voltage induced in the coil as the magnet moves, we use Faraday's law (5). If we perform the following the time derivative of the magnetic flux (11), we obtain for the voltage induced in the collection coils

$$U(t) = -\frac{\mathrm{d}\Phi}{\mathrm{d}t} = 4mC_1A_z\omega\sin(\omega t) = mC\sqrt{2}\sin(\omega t) , \tag{12}$$

where C is the calibration constant of the magnetometer, determined by measuring a known sample.

This arrangement also has the advantage of being insensitive to changes in the external magnetic field. The electromotive voltage induced by a change in the external field is the same in each coil. However, because two and two are connected with opposite polarity, the resulting induced voltage is almost zero, except for variations due to inhomogeneity of the external field and differences between coils.

Figure 3 shows the schematic of the magnetometer used.

By changing the external magnetic field (by changing the current flowing through the electromagnet), we can then measure the magnetization curve of the sample, i.e., the dependence of the sample's magnetic moment on the magnetic field.

Lock-in power supply

We use a so-called lock-in amplifier to suppress circuit noise. This device amplifies the AC component of the measured signal, which has the same frequency as the reference signal. It very effectively suppresses electromagnetic noise at frequencies other than the measured component. This way, we can measure AC voltages in fractions of a microvolt. The reference signal source is a small permanent magnet mounted on a vibrating rod outside the magnet and a reference coil

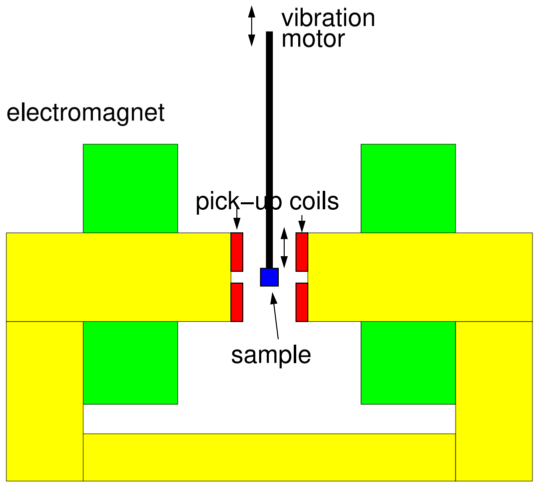

Obrázek 3: Schematic layout of the magnetometer. The iron core of the electromagnet is plotted in yellow, electrical windings in green, collecting coils in red, the sample in blue, and the vibrating rod in black

.

in its vicinity. Thus, the reference signal has the same frequency and phase as the measured signal. It is advisable to use an experimental frequency different from the possible sources of interference; in particular, it is a good idea to avoid multiples of the mains frequency of 50 Hz, and so on.

The lock-in amplifier measures the centered value

$$U_{\rm out} = \frac{1}{T}\int_t^{t+T} U_{\rm in}(\tau)\sin(\omega_{\rm ref}\tau + \phi)\mathrm{d}\tau; , \tag{13}$$

where $U_{\rm in}$ is the input signal, $\omega_{\rm ref}$ is the frequency of the reference signal, ϕ is the tunable phase shift, and T is the selectable time constant of the lock-in amplifier, always much larger than the period of the measured signal. For a harmonic input signal with the same frequency as the reference and zero phase shift, the output voltage is equal to the effective value of the harmonic component of the voltage (amplitude in formula (12) divided by $\sqrt{2}$):

$$U_{\rm lock-in} = Cm, \tag{14}$$

where C is the calibration constant of the magnetometer.

Demagnetization field

For a correct interpretation of the measured data, the demagnetization field in the sample must still be considered. The magnetic field inside the sample H_i, B_i differs from that outside the sample H_e, B_e. The magnetic field near the sample is affected by it and is inhomogeneous. Obviously holds

$$B_e = \mu_0 H_e\ ,\ \ B_i = \mu_0(H_i + M)\ . \tag{15}$$

Furthermore, the continuities of tangential intensity components and normal components at the interface are valid. The solutions are related to the fields inside the sample:

$$H_i = H_e - NM; , \qquad B_i = \mu_0(H_i + M) = B_e + \mu_0(1-N)M\ , \tag{16}$$

where N is the demagnetization factor depending on the shape and orientation of the sample with respect to the magnetic field direction. Some values are given in table 1. In our case, we restrict ourselves to samples from a thin plate with magnetic field orientation in the plane of the plate. The demagnetization factor is negligible, and the correction according to the relation (16) need not be considered.

Tabulka 1: Table of demagnetization factor for some special cases.

field shape	orientation	N
sphere	arbitrary	1/3
thin plate	perpendicular to the plane	1
thin plate	in plane	0
long thin cylinder	along the axis of the cylinder	0
long thin cylinder	perpendicular to the axis	1/2

Magnetic field shielding in a cylindrical cavity

Theory

The magnetic permeability of materials μ expresses the relationship between magnetic induction and magnetic intensity $B = \mu_r \mu_0 H$ and can be studied through magnetic field shielding. For non-ferromagnetic materials, the relative permeability μ_r takes values very close to one, so their response in a magnetic field is not very different from that of a vacuum. The permeability of ferromagnetics is related to the hysteresis curve; the permeability is proportional to the tangent directive to the hysteresis curve. For ferromagnetics, it can take on very high values but depends strongly on the magnitude of the magnetic field. Magnetically soft ferromagnetics (small coercive fields) have high permeabilities, while magnetically hard materials have low permeabilities. Magnetically hard materials have permeabilities in the order of tens to hundreds, while magnetically soft unique materials with high permeabilities can reach values as high as 10^6. We can assume a linear dependence of $B = \mu_r \mu_0 H$ with constant permeability for small magnetic fields and magnetically soft materials.

Magnetic field shielding in a cylindrical cavity

If we place a hollow cylinder of radius R in a homogeneous magnetic field of magnitude B_o perpendicular to the cylinder's axis, the field inside the cylinder is also homogeneous of lower magnitude B_i. The complete calculation is somewhat tedious [3, 2], here we restrict ourselves to stating the assumptions:

- Magnetic intensity and induction satisfy Maxwell's equations in the absence of external currents
$$\mathrm{div}\boldsymbol{B} = 0, \quad \mathrm{rot}\boldsymbol{H} = 0. \tag{17}$$
- A linear material relation relates the magnetic induction and intensity
$$\boldsymbol{B} = \mu_r \mu_0 \boldsymbol{H}. \tag{18}$$
- The tangential component of the magnetic intensity is continuous at the interface of two environments.
- The normal component of magnetic induction is continuous at the interface of two environments.
- The magnetic induction at a large distance r from the cylinder axis is
$$\boldsymbol{B}(r \gg R) = \boldsymbol{B}_o. \tag{19}$$

Figure 4 shows the resulting magnetic field waveform. The ratio of the induction outside B_o to that inside the tube B_i is given by the shielding coefficient S, for which the relation [3, 2]

$$S = \frac{B_o}{B_i} = \frac{(\mu_r + 1)^2 - \frac{b^2}{a^2}(\mu_r - 1)^2}{4\mu_r}, \tag{20}$$

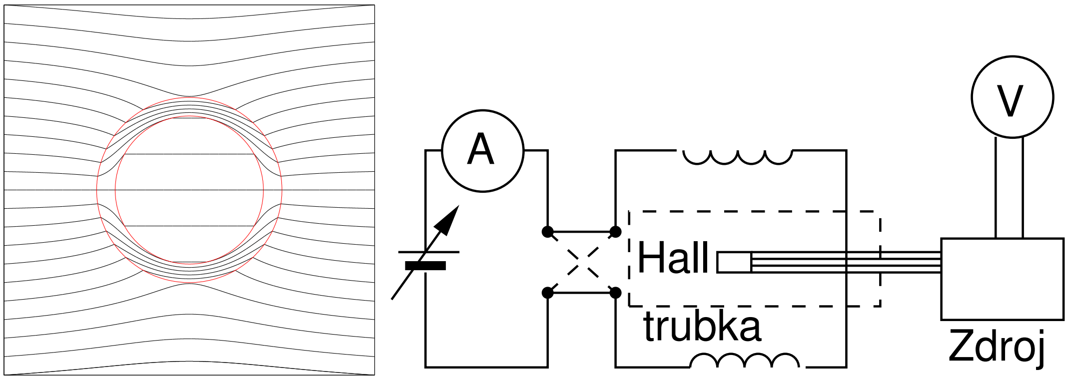

Obrázek 4: Left: The magnetic field lines in and around a hollow cylinder made of ferromagnetic material with permeability $\mu_r = 10$. In the close vicinity of the cylinder, the homogeneity of the magnetic field is somewhat disturbed. Right: Schematic diagram of the Helmholtz coils. The position of the shielding tube and the Hall probe for measuring the magnetic field are indicated.

where a is the outer radius, and b is the inner radius of the hollow cylinder. For high values of magnetic permeability $\mu_r \gg 1$ and the small wall thickness of the tube d relative to its radius $d \ll R$, we can use the approximate relation

$$S = \frac{B_o}{B_i} \approx 1 + \frac{\mu_r d}{2R}. \tag{21}$$

The above relations hold for small magnetic fields. Especially inside materials with high permeability, the maximum value of the magnetic induction (approximately equal to $B_{\max} \approx \mu_r B_o$) can easily exceed the saturation magnetization of the material (for iron about 2.2 T), and the overall shielding coefficient then comes out effectively lower. This property appears as a dependence of the shielding coefficient on the external field, which decreases with a larger external field. The low-field permeability value is obtained from the low-field shielding coefficient values, where the shielding coefficient is independent of the field strength.

Homogeneous magnetic field in Helmholtz coils

Helmholtz coils are the simplest way to create a homogeneous field. These are two coils of the same number of turns and radius R placed on a common axis at a distance of their radius R from each other. The magnetic field of one coil can be calculated using the Biot-Savart law

$$\boldsymbol{H} = \int \frac{I}{4\pi r^3} \boldsymbol{r} \times \mathrm{d}\boldsymbol{l}, \tag{22}$$

where I is the current flowing through the conductor, r is the distance of the length element $\mathrm{d}\boldsymbol{l}$ from the field measurement point. The magnetic field on the axis of a narrow coil of radius R with N turns at a distance z from the center of the coil is easily calculated as

$$H(z) = \frac{NIR^2}{4\pi(R^2 + z^2)^{3/2}} \int_0^{2\pi} \mathrm{d}\varphi = \frac{NIR^2}{2(R^2 + z^2)^{3/2}}. \tag{23}$$

The magnitude of the magnetic in the center of the cavity of the Helmholtz coils is obtained as the sum of the contribution of both coils (the distance of the center of the cavity from the center of each coil is $z = R/2$)

$$H = 2\frac{NIR^2}{2(R^2 + (R/2)^2)^{3/2}} = \left(\frac{4}{5}\right)^{3/2} \frac{NI}{R}. \tag{24}$$

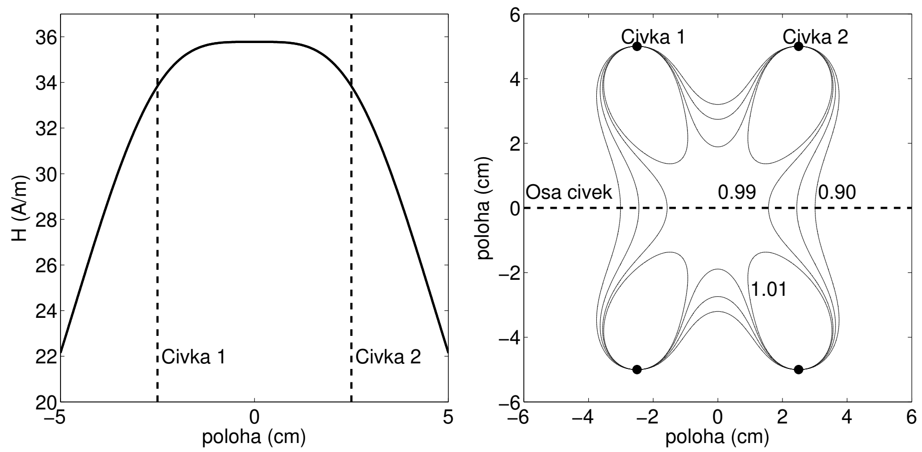

Obrázek 5: Left: Magnetic field strength on the axis of Helmholtz coils with radius $R = 5\,\mathrm{cm}$. Right: Distribution in the plane of the axis of Helmholtz coils. Shown are the contours for the 0.90, 0.95, 0.99, and 1.01 values at the center of the cavity. In the star-shaped region's center region, the magnetic field magnitude deviation is less than 1%.

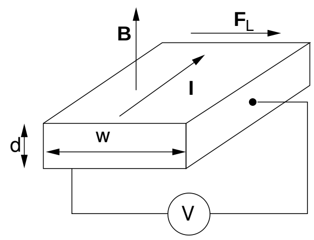

Obrázek 6: The principle of the Hall effect.

Hall probe magnetic field measurements

Use the Hall effect to measure the magnitude of the magnetic field. When charge carriers in a sample move in a magnetic field (electrons or holes in a semiconductor), the Lorentz force acts on them perpendicular to the direction of their motion

$$\boldsymbol{F}_L = q\boldsymbol{v}_d \times \boldsymbol{B}, \tag{25}$$

where q is their charge and $\boldsymbol{v}_d$ is their drift velocity. In the steady state, an electric field $\boldsymbol{E}_H$ is generated, which eliminates the effect of the Lorentz force

$$\boldsymbol{F}_H = q\boldsymbol{E}_H = -\boldsymbol{F}_L. \tag{26}$$

We substitute the drift velocity $v_d = \frac{j}{nq} = \frac{1}{nq}\frac{I}{wd}$, where j is the current density, n the concentration of charge carriers, d the thickness and w the width of the sample. Then, by comparing these relations, we get the relation for Hall stress

$$U_H = E_H w = \frac{R_H}{d} I\ B, \tag{27}$$

where $R_H = \frac{1}{nq}$ is the Hall constant and d is the sample thickness. The sign of the Hall constant corresponds to the sign of the charge carriers, thus allowing us to determine the conductivity type and measure the charge carriers' concentration. Conversely, a Hall probe of known parameters can measure magnetic induction. We will use a commercial Hall probe with integrated current source and amplifying electronics of unknown parameters.

Measurement progress

Make a magnetic field measurement without the tube inserted, and measure the Hall voltage U_o proportional to the external magnetic field B_o. With the tube inserted, measure the voltage U_i proportional to the magnetic induction inside the tube B_i. The shielding coefficient S is equal to the fraction of the voltage

$$S = \frac{U_o}{U_i}. \tag{28}$$

To eliminate any possible mids-setting of the zero (zero voltage may not correspond to a state without a magnetic field), we make measurements for both commutations of the current (+ and −) and then average the resulting voltage concerning the sign

$$U = \frac{1}{2}\left(U_+ - U_-\right). \tag{29}$$

Úkoly

1. Plug the Helmholtz coils into the circuit.
2. Measure the shielding coefficient S and the dimensions of the set of cylindrical tubes provided. Measure the external field B_o at the center of the cavity without the shielding tube inserted and the value of B_i after the shielding tube is inserted. Make measurements for several current values through the coils (recommended values of 0.5 A, 1.5 A and 2.5 A) and see if the shielding coefficient is independent of the external field strength. Measure for both directions of the current commutation.
3. Calculate their permeability using the relation (21) or (20).

Recommended procedure and tasks for measurements

The student has three weeks to make the measurements. Recommended procedure:

- First week – familiarization with the magnetometer; calibration of the magnetometer using a reference sample (nickel plate).
- Second and third week – measuring the magnetization curve for several samples according to the target.

The output of the practicum will be presented to the instructor in the form of graphs and measured dependencies, including an estimate of uncertainties where possible and appropriate

Reference

[1] D. Griffith, *Introduction to electrodynamics*, Prentice-Hall (1999).

[2] J.D. Jackson: *Classical electrodynamics*, Willey (1999).

[3] J. Perry, Proc. Phys. Soc. London **13**, 227 (1894).